

1  
2  
3  
4  
5  
6  
7  
8  
9  
10  
11  
12  
13  
14  
15  
16  
17  
18  
19  
20  
21  
22  
23

# AN ADAPTIVE FORMULATION OF THE SMOOTH VARIABLE STRUCTURE FILTER BASED ON STATIC MULTIPLE MODELS

## Abstract

The Kalman filter (KF) is the most well-known estimation strategy that yields the optimal solution to the linear quadratic estimation problem. The system in such applications shall be well modeled assuming the presence of Gaussian noise. While the KF is effective under the stated conditions, it lacks robustness to other type of disturbances. Therefore, numerous variants of the KF have been developed to accommodate its limitations. The smooth variable structure filter (SVSF) is as an alternative solution with improved robustness, especially in the case of modeling uncertainties. It is based on sliding mode technique that offers robustness at the cost of optimality. On the other hand, some algorithms and solutions involve with several possible operating modes and generates an estimation based on the output of these models, i.e. the static multiple models that obtains the estimates based on weighted statistical fusing of the outputs of the models depending on the likelihood of each mode. This paper introduces an adaptive formulation of the SVSF that is reformulated based on static multiple models. The proposed model is applied and tested on an electro-hydrostatic actuator (EHA). The proposed method takes the advantages of the SVSF's robustness and stability, while reducing the estimation error due to the use of adaptive modeling structure. The results show an improvement on the SVSF performance, where the root mean squared errors are reduced by 41%, 99% and 75% for the position, velocity and acceleration

24 estimated states. Therefore, the proposed method is a good candidate for parameter and state  
 25 estimation problems.

26 **Keywords:** State and parameter estimation; Kalman filter; smooth variable structure filter;  
 27 robustness; static multiple models

28 **Table of Nomenclature**

Symbols	Representation	Symbols	Representation
$\circ$	Schur Product	$\gamma$	SVSF Coefficient Matrix
$X^+$	Pseudoinverse of $X$	$\psi$	Boundary layer vector
$X^{-1}$	Inverse of $X$	$z_k$	measurement value at time $k$
$\hat{X}$	Estimated value of $X$	$P$	Error covariance matrix
$ X $	Absolute value of $X$	$Q$	System noise's covariance matrix
$A$	System Matrix	$R$	Measurement noise's covariance matrix
$B$	Input Matrix	$x$	State Vector
$C$	Measurement Matrix	$z$	Measurement Vector
$X_{k k}$	The a posteriori vale of $X$ at time $k$	$e_z$	Error in measurement.
$X_{k k-1}$	The a priori vale of $X$ at time $k$	$K_k$	Correction gain at time $k$
$u_k$	Input value at time $k$	$M^j$	Model $j$ structure.
$\mu_k^j$	Weight at time $k$ for each model $M^j$	$T$	The time step, 1 msec.
$\sigma_j^2$	The variance of model $M^j$	$sat$	Saturated function
$sgn$	Sign function	$r$	Number of models for SSM
$n, m$	Number of states and measurements, respectively.	$diag$	Convert the vector to a diagonal matrix where the elements of the vector are the diagonal elements of the matrix.

29

30 **1. Introduction**

31 Estimating the dynamic behavior involves the extraction of important values known as states from  
 32 noisy measurements [1, 2]. States change over time and are typically governed by equations that  
 33 describe system dynamics [3]. The estimation process is referred to as Filter as it tries to minimize  
 34 the noise effect. Most of filters try to minimize the error (difference between the actual and  
 35 estimated state values) while simultaneously reducing the effects of noise. The other type of filters  
 36 try being robust to disturbances [3]. Disturbances and noise are typically present in measurements,

37 and may be caused by the sensor quality (system uncertainties) as well as environmental factors  
38 (Measurement uncertainties). System uncertainties may be caused by an inaccurate model and/or  
39 variations and nonlinearities in the physical system parameters. Reliable estimates of state and/or  
40 parameters are necessary for safely and accurately controlling a system in real-time. When system  
41 dynamics are changed abruptly in the presence of faults, adaptive estimation strategies that  
42 combined both types of filters can be used to mitigate inaccurate estimation. They maintain the  
43 stability of the filter during the fault, while reducing the error in the estimation.

44 Kalman expanded on the research of his predecessors and introduced a new solution to  
45 linear filtering and tracking problems [4]. He derived a filter that utilized linear models and  
46 measurements to yield an optimal estimation based on strict assumptions. This filter later became  
47 known as the Kalman filter (KF). Since the KF is applicable to linear Gaussian models, several  
48 works were conducted to modify the KF and make more applicable to nonlinear and/or non  
49 Gaussian models, i.e. Extended KF, and Unscented KF [4].

50 Another branch of estimation methods is still developing in parallel to the KF and its  
51 variants. This branch includes the well-known sliding mode observers (SMOs). These observers  
52 are based on variable structure (VS) and sliding mode (SM) techniques [5, 6, 7]. Both techniques  
53 consider the system has discontinuity in his structure. Therefore, they define discontinuities  
54 hyperplanes that divide the state space into different regions; within these regions, the equations  
55 used to describe the system are continuous [8, 9]. The name ‘variable structure’ is chosen since  
56 system dynamics may be mathematically described by a finite number of equations.

57 Variable structure theory provided the foundation for variable structure control (VSC). In  
58 VSC, the controller signal is formulated as a discontinuous state function, such that discontinuity  
59 hyperplanes are introduced [8, 9]. The most well-known type of VSC is the sliding mode controller

60 (SMC) [6, 10]. SMC makes use of a discontinuous switching plane along a desired state trajectory,  
61 which is referred to as the sliding surface. The primary objective for the SMC is to maintain the  
62 states within sliding surface neighbourhood. A switching gain is used to push the states towards  
63 the surface when they try to move away. Once the state values are on the surface, the states slides  
64 along the surface towards the desired values [10]. Although the switching effects bring robustness  
65 and stability to the control process, it also introduces high-frequency switching known as  
66 chattering [11]. Quite often a boundary layer is introduced in an effort to smooth out the control  
67 signal [10]. Prior to the 1980s, VSC and SMC methods were only considered in the continuous-  
68 time domain [12]. In 1985, a discrete-time formulation of SMC was presented [13]. A stability  
69 condition was provided shortly afterwards and is now typically used in the design of discrete  
70 controllers [14, 15].

71 SMOs, which was developed in 1980s [12, 16], reduces the error with the help of a  
72 switching function similar to VSC and SMC [17]. Observer gains are calculated based on the errors  
73 between the measurements and estimates [17]. Most SMOs apply a discontinuous signal to the  
74 estimates in order to keep them bounded to an area of the surface [12]. The motion consists of  
75 three phases: reachability, injection, and sliding [12, 18]. The reachability phase consists of forcing  
76 the estimates to the sliding surface from some initial conditions, in a finite period of time [12].  
77 Once within a defined area of the surface (called an existence subspace), both the injection and  
78 sliding phases are present. The sliding phase forces the estimated errors to slide along a hyperplane  
79 towards the origin [12]. The injection phase consists of preventing the estimate from leaving the  
80 existence subspace; keeping it bounded within an area of the sliding surface [12]. According to  
81 [12, 16, 19], the action of the injection phase enables the observer to be robust enough to overcome  
82 uncertainties, modeling errors, and nonlinearities present in the system. A number of SMOs have

83 been developed based on these principles. The most notable observers were introduced by Slotine  
84 et al. [9, 20], Walcott et al. [21, 22], Edwards et al. [19], and later by both Tan and Edwards [23].  
85 SMOs have been applied to estimation problems, and fault detection and isolation [12].

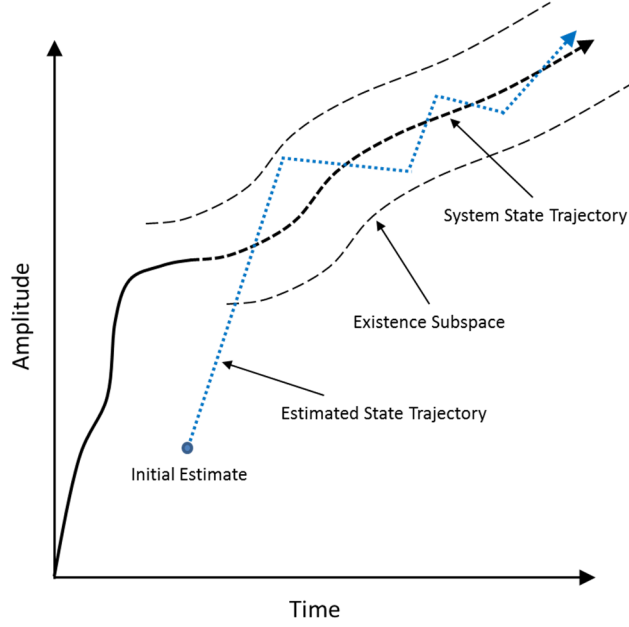
86 Another filter called the smooth variable structure filter (SVSF) was presented in 2007,  
87 which was based on sliding mode and variable structure techniques [3, 12, 24]. The SVSF is  
88 formulated as a predictor-corrector estimator similar to the KF. However, it utilizes a gain structure  
89 based on sliding mode techniques. The filter's gain is calculated based on the error in  
90 measurements at the prediction stage of the current time (known as innovation), the error in  
91 measurements at the update stage from the previous time step, and a switching term [24]. Similar  
92 to SMOs, the switching gain structure improves stability and robustness of the estimation process  
93 by bounding the state estimates close to the true trajectory [25, 26]. The SVSF presented in [24]  
94 did not contain a state error covariance derivation, which is an important feature for optimal  
95 estimation strategies (it is another performance indicator). A state error covariance function was  
96 introduced and expanded in [25, 27, 28], which vastly improved the number of useful applications  
97 for the SVSF [29, 30, 31]. Other developments and improvements to the SVSF were conducted in  
98 the literature including fault detection using chattering, higher-order implementations, and  
99 tracking multiple targets [12, 32, 33, 34, 35]. The SVSF has demonstrated robust performance on  
100 a number of different estimation problems [4]. Most recently, a filter, which is referred to as the  
101 sliding innovation filter (SIF), was introduced in [36, 37, 38, 39]. The SIF is based on similar  
102 concepts to the SVSF, but offers a simpler formulation with improved results. An opportunity for  
103 improving the SVSF involves the development of an adaptive formulation. The ability for the  
104 SVSF to automatically modify its system and/or measurement models based on different operating  
105 modes offers significant room for improvement (e.g., in terms of both accuracy and robustness).

106 In this paper, a new adaptive formulation of the SVSF is presented and tested on an  
107 experimental setup. The novel method integrates the static multiple models estimator (SMM) with  
108 the SVSF predictor-corrector estimation strategy. The SMM consists of several possible operating  
109 modes where several possible estimates are obtained. The SMM then combines these estimates  
110 using some weights based on the likelihood of each mode. This strategy may be used for fault  
111 detection and diagnosis problems, and has demonstrated good accuracy and repeatability of results.  
112 The performance of the proposed method is evaluated using an electro-hydrostatic actuator (EHA)  
113 which was built for experimentation. The results are compared with the standard SVSF estimation  
114 method.

115 This paper is organized as follows. Section 2 summarizes the SVSF estimation process.  
116 Section 3 introduces the SMM estimator and the proposed SMM-SVSF or the adaptive SVSF  
117 algorithm. Section 4 describes the experimental setup as well as the equations of motion governing  
118 the EHA. Section 5 discusses the application of the standard SVSF and adaptive SVSF to the EHA  
119 system, followed by concluding remarks.

## 120 **2. The Smooth Variable Structure Filter**

121 The smooth variable structure filter (SVSF) is a predictor-corrector estimation strategy that  
122 offers solution with robustness and stability against disturbances and uncertainties. The SVSF uses  
123 a smoothing boundary layer with an upper bound that is defined based on the level of noise and  
124 unmodeled dynamics [40, 41]. The SVSF is model-based and may be applied to both linear or  
125 nonlinear systems and measurements [3, 12]. The SVSF's concepts are illustrated in Fig. 1.



126

127

**Figure 1.** SVS's concepts with existence subspace boundary layer [3].

128

129

As described earlier, the SVSF strategy is structured similarly to the KF. However, it presents a novel way to calculate its gain. As per (2.1) and (2.2),  $\hat{x}_{k+1|k}$  and  $P_{k+1|k}$  are calculated.

130

$$\hat{x}_{k+1|k} = A\hat{x}_{k|k} + Bu_k \quad (2.1)$$

131

$$P_{k+1|k} = AP_{k|k}A^T + Q_k \quad (2.2)$$

132

Then  $\hat{z}_{k+1|k}$  and  $e_{z,k+1|k}$  are calculated as per (2.3) and (2.4), respectively.

133

$$\hat{z}_{k+1|k} = C\hat{x}_{k+1|k} \quad (2.3)$$

134

$$e_{z,k+1|k} = z_{k+1} - \hat{z}_{k+1|k} \quad (2.4)$$

135

136

The gain used by the SVSF,  $K_k$ , is calculated with the use of the boundary layer widths,  $\psi$ , as follows [3]:

137

$$K_{k+1} = C_k^+ \text{diag} \left[ \left( |e_{z_{k+1|k}}| + \gamma |e_{z_{k|k}}| \right) \circ \text{sat} \left( \bar{\psi}^{-1} e_{z_{k+1|k}} \right) \right] \text{diag} \left( e_{z_{k+1|k}} \right)^{-1} \quad (2.5)$$

138 The saturation function is defined as follows:

$$139 \quad \text{sat} \left( \bar{\psi}^{-1} e_{z_{k+1}|k} \right) = \begin{cases} 1, & e_{z_i, k+1|k} / \psi_i \geq 1 \\ \frac{e_{z_i, k+1|k}}{\psi_i}, & -1 < \frac{e_{z_i, k+1|k}}{\psi_i} < 1 \\ -1, & e_{z_i, k+1|k} / \psi_i \leq -1 \end{cases} \quad (2.6)$$

140 where  $\bar{\psi}^{-1}$  is defined by (2.7) for  $m$  number of measurements [3]:

$$141 \quad \bar{\psi}^{-1} = \begin{bmatrix} \frac{1}{\psi_1} & 0 & 0 \\ 0 & \ddots & 0 \\ 0 & 0 & \frac{1}{\psi_m} \end{bmatrix} \quad (2.7)$$

142 The state vector and error covariance matrix are respectively updated as per (2.8) and (2.9).

$$143 \quad \hat{x}_{k+1|k+1} = \hat{x}_{k+1|k} + K_{k+1} e_{z, k+1|k} \quad (2.8)$$

$$144 \quad P_{k+1|k+1} = (I - K_{k+1} C) P_{k+1|k} (I - K_{k+1} C)^T + K_{k+1} R_{k+1} K_{k+1}^T \quad (2.9)$$

145 Finally, the updated measurement error,  $e_{z, k+1|k+1}$ , is found as per (2.10) and is used in the next  
146 iteration.

$$147 \quad e_{z, k+1|k+1} = z_{k+1} - \hat{z}_{k+1|k+1} \quad (2.10)$$

148 The existence subspace, denoted by the dotted black line shown in Figure 1, refers to the  
149 level of uncertainty found in the estimation process. It is typically present due to the amount of  
150 noise and/or modeling uncertainties [3]. The existence space,  $\beta$ , is described mainly from the  
151 innovation signal [27, 34]. While the width is not precisely known, designer knowledge may be  
152 used to define the upper bound. When the smoothing boundary is defined larger than the existence  
153 subspace, the estimated states are smoothed. Likewise, if the smoothing term is set too small,  
154 chattering (high-frequency switching) may occur.

155 **3. A Novel Adaptive Formulation of the Smooth Variable Structure Filter**

156 The static multiple model (SMM) algorithm assumes that the system behaves according to  
 157 a finite number of  $r$  models  $M^1, M^2, \dots, M^r$ . The SMM uses variable weights,  $\mu_k^j$ , calculated at  
 158 time  $k$  to represent each model  $M^j$ . These weights represent a probability of the system behaving  
 159 according to a corresponding operating mode (i.e., mathematical model). These weights are used  
 160 to combine the corresponding model state estimates [42] which creates an overall estimate. The  
 161 weights are initially uniformly distributed, and subsequent weights are calculated as follows:

162 
$$\mu_k^j = \frac{p(z_k|M^j)\mu_{k-1}^j}{\sum_{i=1}^r p(z_k|M^i)\mu_{k-1}^i} \quad (3.1)$$

163 where  $p(z_k|M^j)$  is the likelihood value of measurement  $z_k$  based on  $M^j$  and is defined as follows:

164 
$$p(z_k|M^j) = \frac{1}{\sqrt{2\pi\sigma_j^2}} \exp \frac{-(z_k - \hat{z}_{k|k-1})^2}{2\sigma_j^2} \quad (3.2)$$

165 
$$\sigma_j^2 = C_k^j P_{k|k-1}^j C_k^{jT} + (\sigma_z^2)^j \quad (3.3)$$

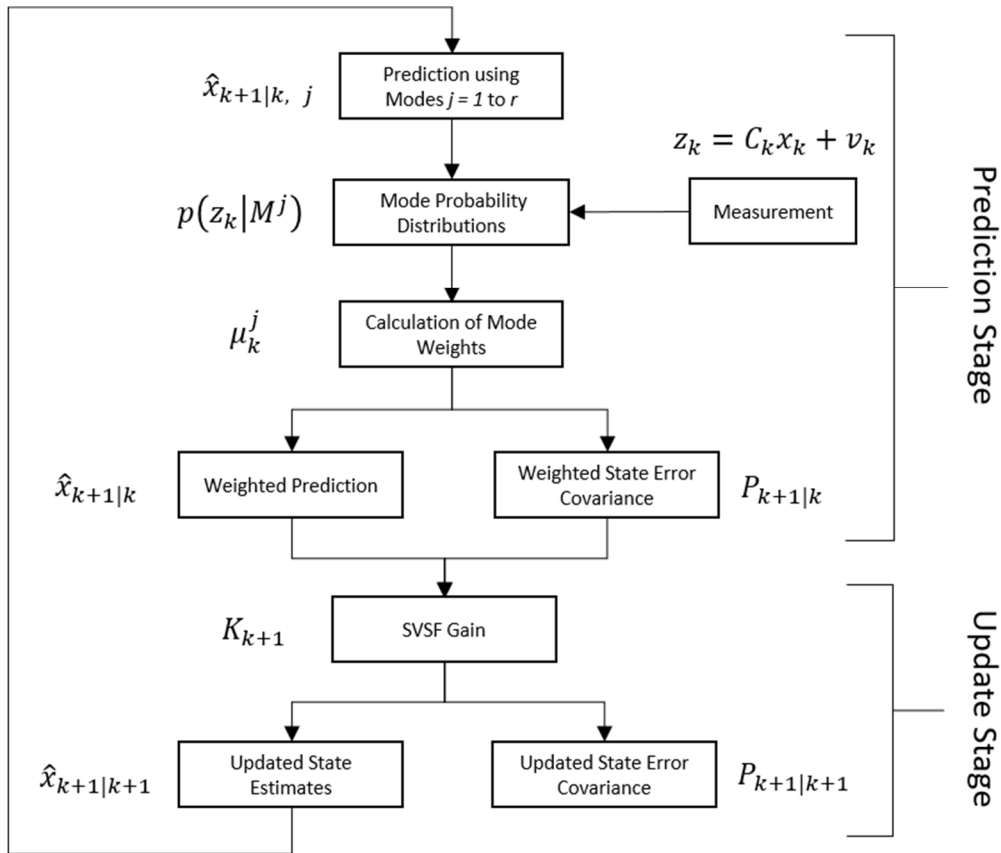
166 where  $\sigma_j^2$  refers to the variance of model  $M^j$  based on the predicted measurement  $\hat{z}_{k|k-1}$  for model  
 167  $M^j$  [42]. Note that the parameter definitions may also be found in the Table of Nomenclature. Each  
 168 model has its own likelihood value calculated from the filtering strategy (whether it is from a  
 169 Kalman filter, smooth variable structure filter, or another type). The adaptive estimates are  
 170 calculated using the weighted sum produced by the system models, as per (3.4).

171 
$$\hat{x}_{k|k} = \sum_{j=1}^r \mu_k^j \hat{x}_{k|k}^j \quad (3.4)$$

172 The adaptive covariance is calculated in a similar fashion, as shown in (3.5).

$$173 \quad P_{k|k} = \sum_{j=1}^r \mu_k^j \left[ P_{k|k}^j + (\hat{x}_{k|k}^j - \hat{x}_{k|k}) (\hat{x}_{k|k}^j - \hat{x}_{k|k})^T \right] \quad (3.5)$$

174 The proposed SMM-SVSF (or adaptive SVSF) uses the model weights from the static  
 175 multiple models estimator to generate a weighted prediction. The weighted state predictions are  
 176 used to calculate the SVSF gain, which is used to generate an updated state estimate and state error  
 177 covariance. Since the algorithm uses a weighted combination of system modes, the weights could  
 178 be used to describe the mixing of different system modes. Figure 2 depicts the algorithm flow chart  
 179 and Table 1 shows the corresponding pseudocode. Note that the initial mode weights can be  
 180 defined by the user, provided that the sum of each value is 1 (so total probability is 100%).



181

182 **Figure 2.** The proposed SMM-SVSF (or adaptive SVSF) flowchart.

183 **Table 1.** Pseudocode for the SMM-SVSF algorithm.

1:	For models $(M^j)$ , $j = 1$ to $r$
	$\hat{x}_{k+1 k,j} \leftarrow (A_j, u)$
2:	For models $(M^j)$ , $j = 1$ to $r$
	$\sigma \leftarrow (Q, R, P_{k k})$
	$p \leftarrow (\hat{x}_{k+1 k,j}, z, \sigma)$
3:	$\mu_{k+1} \leftarrow (\hat{x}_{k+1 k,j}, \mu_k)$
4a:	$\hat{x}_{k+1 k} \leftarrow (\hat{x}_{k+1 k,j}, \mu_{k+1})$
4b:	For operating modes $j = 1$ to $r$
	$P_{k+1 k,j} \leftarrow (A_j, \hat{x}_{k+1 k})$
5:	$P_{k+1 k} \leftarrow (P_{k+1 k,j}, \mu_{k+1})$
6:	$K_{k+1} \leftarrow (C, \gamma, \text{saturation})$
7a:	$\hat{x}_{k+1 k+1} \leftarrow (\hat{x}_{k+1 k}, z, C, K_{k+1})$
7b:	$P_{k+1 k+1} \leftarrow (P_{k+1 k}, C, K_{k+1}, R)$

184

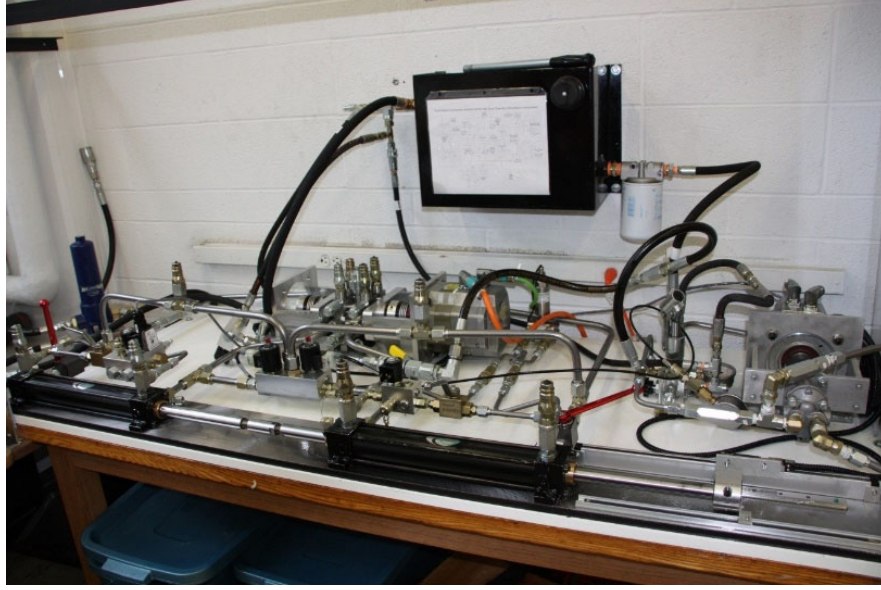
185 After the SVSF boundary layer vector and convergence rate have been set and model  
 186 weights have been initialized, a predicted state estimate for each system model is made. The  
 187 standard deviation is calculated using three different covariance matrices: the state error, the  
 188 system noise, and the measurement noise covariance matrices. Next, the updated estimates,  
 189 standard deviations, and measurements are used to calculate the model probabilities. These  
 190 probabilities are then used to update the model weights, which then are used to generate a weighted  
 191 predicted state estimate and error covariance. This information is fed through the SVSF update  
 192 stage as described in Section 2 using (2.8) through (2.10).

#### 193 **4. Experimental Setup**

194 Electrohydrostatic actuators (EHAs) are a type of hydraulic and electrical actuator  
 195 comprised of a linear or rotary actuator, a hydraulic circuit, and a bidirectional pump [43]. EHAs  
 196 are used in automotive and aerospace industry due to their large force-to-weight ratios and their  
 197 reliability. They are also used in various manufacturing applications such as metal forming, where

198 control of the outlet pressure is required [44]. Electromechanical systems often function under  
199 different operating modes. In the case of the EHAs, faults such as internal leakage and increased  
200 friction may be present. Internal leakage is caused by wearing of the piston seal, which affects the  
201 overall actuation performance [45]. If the leakage remains undetected, then it cannot be repaired,  
202 which can deteriorate lifetime performance and increase maintenance costs [45]. Since detection  
203 of internal leakage in EHAs through disassembly of the cylinder and piston is costly, adaptive  
204 estimation strategies can be used to improve the overall estimation process in the presence of  
205 multiple operating modes.

206         The EHA model used in this paper was designed and manufactured at the Centre for  
207 Mechatronics and Hybrid Technology at McMaster University shown in Figure 3 [43]. The EHA  
208 used in this study is composed of several components, including: two linear actuators, a bi-  
209 directional external gear pump, a variable-speed servomotor, an accumulator, a pressure relief  
210 valve, and safety circuits [46]. A variable-speed brushless DC electric motor drives the pump and  
211 forces hydraulic oil into the cylinder, and modifies the actuation performance by varying the fluid  
212 flow rate. An accumulator is used to prevent cavitation and collect leakages from the gear pump.  
213 The EHA is controlled by modifying input voltage to the motor, which consequently changes the  
214 direction and speed of the pump. Controlling the fluid flow rate in the outer circuit adjusts the  
215 position of the piston, which could be used for aerospace applications such as changing flight  
216 surfaces.



217

218 **Figure 3.** Prototype of the EHA used to collect experimental data [43].

219 The EHA was modelled using four states: the actuator position  $x_1 = x$ , velocity  $x_2 = \dot{x}$ ,  
 220 acceleration  $x_3 = \ddot{x}$ , and differential pressure across the actuator  $x_4 = P_1 - P_2$ . The physical  
 221 modeling approach was used to obtain the nonlinear state-space equations in discrete-time  
 222 described by [3, 47]:

223 
$$x_{1,k+1} = x_{1,k} + Tx_{2,k} \quad (4.1)$$

224 
$$x_{2,k+1} = x_{2,k} + Tx_{3,k} \quad (4.2)$$

225 
$$\begin{aligned} x_{3,k+1} = & 1 - \left[ T \frac{a_2 V_0 + M \beta_e L}{M V_0} \right] x_{3,k} - T \frac{(A_E^2 + a_2 L) \beta_e}{M V_0} x_{2,k} \dots \\ & \dots - T \frac{2 a_1 V_0 x_{2,k} x_{3,k} + \beta_e L (a_1 x_{2,k}^2 + a_3)}{M V_0} \operatorname{sgn}(x_{2,k}) + T \frac{A_E \beta_e}{M V_0} u \end{aligned} \quad (4.3)$$

226 
$$x_{4,k+1} = \frac{a_2}{A_E} x_{2,k} + \frac{(a_1 x_{2,k}^2 + a_3)}{A_E} \operatorname{sgn}(x_{2,k}) + \frac{M}{A_E} x_{3,k} \quad (4.4)$$

227 The system input is defined as follows:

228 
$$u = D_p \omega_p - \text{sgn}(P_1 - P_2) Q_{L0} \quad (4.5)$$

229 where  $\omega_p$  is the pump speed. Table 2 summarizes and defines the numeric values of the parameters  
 230 in the equations (4.1) to (4.5).

231 **Table 2.** The EHA parameters, definitions, and values used in the experiment.

232

Parameter	Description	Parameter Values
$A_E$	Piston Area (m <sup>2</sup> )	$1.52 \times 10^{-3}$
$D_p$	Pump Displacement ( m <sup>3</sup> /rad )	$5.57 \times 10^{-7}$
$L$	Leakage Coefficient ( m <sup>3</sup> /(s×Pa))	$4.78 \times 10^{-12}$
$M$	Load Mass (kg)	7.376 kg
$Q_{L0}$	Flow Rate Offset ( m <sup>3</sup> /s)	$2.41 \times 10^{-6}$
$V_0$	Initial Cylinder Volume ( m <sup>3</sup> )	$1.08 \times 10^{-3}$
$\beta_e$	Effective Bulk Modulus (Pa)	$2.07 \times 10^8$
$a_1$	Friction Coefficient	$6.589 \times 10^4$
$a_2$	Friction Coefficient	$2.144 \times 10^3$
$a_3$	Friction Coefficient	436

236

237 The friction was modeled using a quadratic function based on the actuator velocity. The  
 238 friction coefficients were obtained by performing experiments ranging from 15.6 to 109 radians  
 239 per second with each data set containing four trials for repeatability [43].

240 **5. Results and Discussion**

241 The results of applying the proposed strategy on the EHA is discussed in this section. The  
 242 state estimates were initialized to zero and the covariance matrices for system and measurement  
 243 noises were defined respectively as  $Q = 10^{-9}I_{4 \times 4}$  and  $R = 10^{-6}I_{4 \times 4}$ , where  $I$  is an identity matrix.  
 244 Furthermore, the state error covariance matrix  $P$  was initialized as  $10Q$ .

245 Leakage faults were introduced to investigate the effects of parametric uncertainties in the  
 246 system. The purpose of this study was to demonstrate the efficiency of the proposed strategy  
 247 compared to the standard SVSF. The SMM-SVSF algorithm demonstrates robustness in the

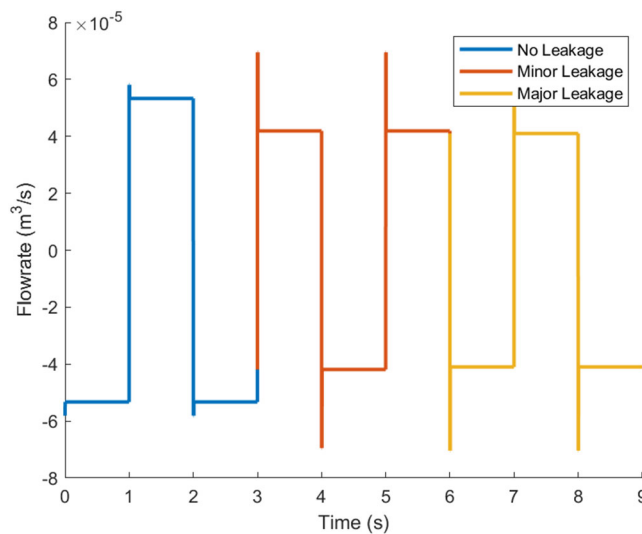
248 presence of multiple operating modes. Multiple system modes are introduced to the system in the  
 249 form of leakage faults. In order to obtain the coefficients of the leakage values, the EHA was  
 250 operated with a constant pump speed of 94.25 radians per second under a series of differential  
 251 pressures. The differential pressure was modified using a throttling valve in the hydraulic system.  
 252 To ensure repeatability, five sets of measurements were made. A linear regression was performed  
 253 on each data set, and the slope and intercept were used to define  $L$  and  $Q_{L0}$ , respectively. The  
 254 leakage coefficients and flow rate offsets used for this study are presented in Table 3.

255 **Table 3.** Leakage coefficient values and flow rate offsets for varying operating conditions.

Condition	Leakage, $L$ , ( $\text{m}^3/(\text{s}\times\text{Pa})$ )	Flow Rate Offset, $Q_{L0}$ , ( $\text{m}^3/\text{s}$ )
Normal	$4.78 \times 10^{-12}$	$2.41 \times 10^{-6}$
Minor Leakage	$2.52 \times 10^{-11}$	$1.38 \times 10^{-5}$
Major Leakage	$6.01 \times 10^{-11}$	$1.47 \times 10^{-5}$

256

257 A minor leakage is introduced to the system at  $t = 3 \text{ sec}$  and a major leakage is  
 258 introduced at  $t = 6 \text{ sec}$ . The effect on the input flow rate can be seen in Figure 4.

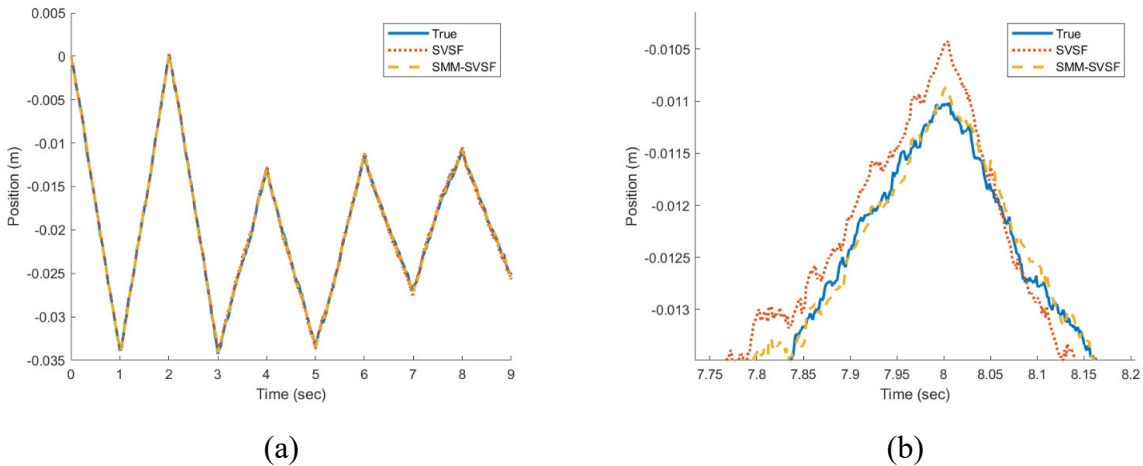


259

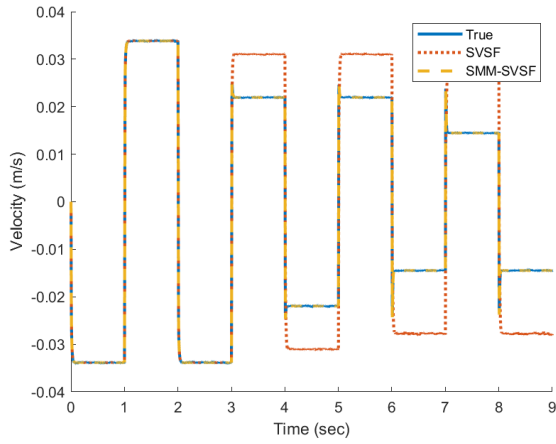
260 **Figure 4.** Input flow rate due to internal leakage faults.

261 Once the EHA was modeled at all these operations and they were verified experimentally,  
 262 we used these mathematical models and values in a Matlab Simulation to compare the performance  
 263 between the proposed algorithm to the traditional one. The benefits of using the simulation can be  
 264 summarized in two points; the values at certain point are known, i.e. the true state, and the  
 265 prototype will not be damaged due to the fault when introduced. The results of the simulation are  
 266 shown in Figure 5 to Figure 8 and table 5.

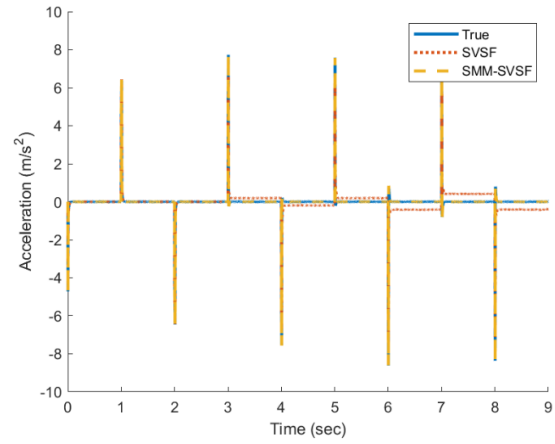
267 Figure 5 shows the position estimates, while the velocity and acceleration estimates are  
 268 shown in Figure 6a and 6b, respectively. The SMM-SVSF performs slightly better than the  
 269 classical SVSF when the major leakage fault is introduced as seen in Figures 5a and 5b. The SVSF  
 270 filter shows a significant deviation from the true velocity when the minor leakage fault is  
 271 introduced at 3 seconds, as shown in Figure 6a. The error becomes worse when the major leakage  
 272 is introduced at 6 seconds as shown in Figure 6b. This error is caused by the modeling uncertainty  
 273 of the acceleration state, particularly due to flow rate offset of the input. The greatest improvement  
 274 can be seen in the velocity and acceleration estimates. Overall, the SMM-SVSF greatly  
 275 outperforms the classical SVSF in the presence of modeling uncertainties such as leakage faults.



276 **Figure 5.** Position estimates with leakage faults:  
 277 (a) 9 second simulation, (b) zoomed in at 8 seconds (major leakage).



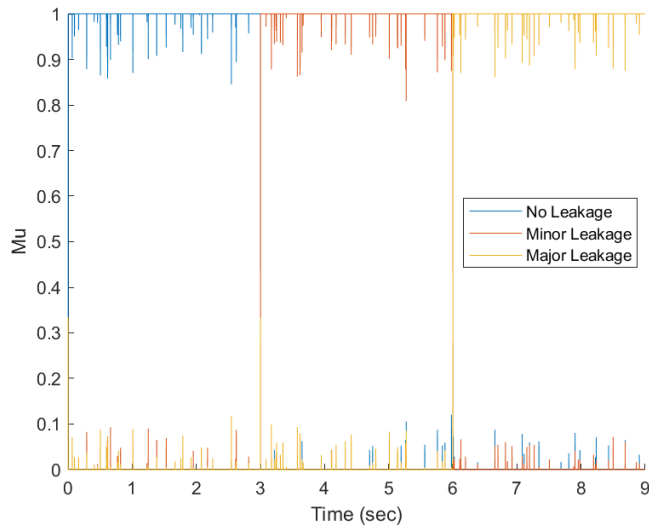
(a)



(b)

278  
279

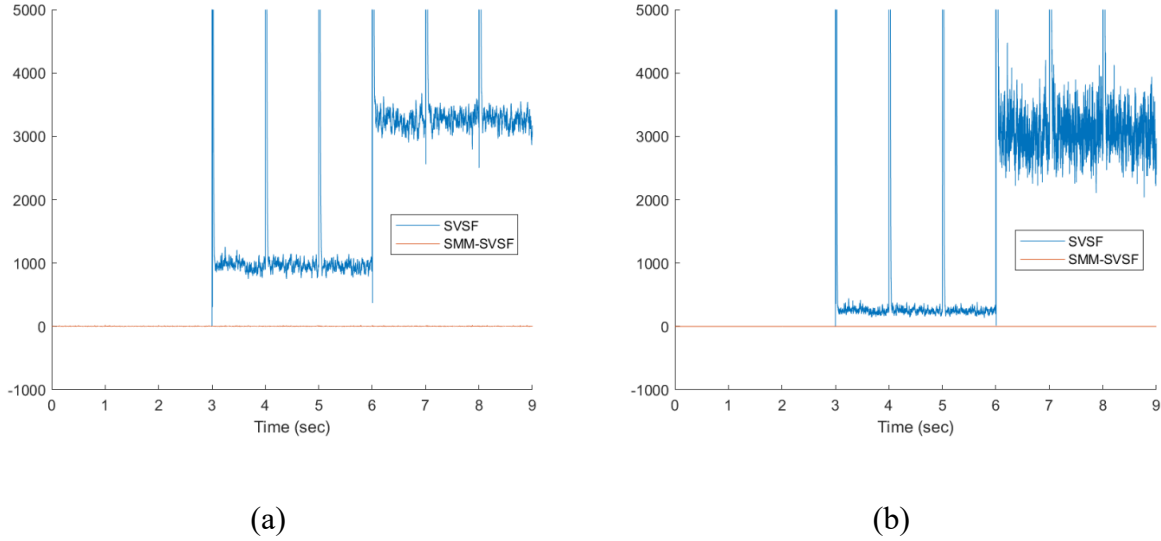
**Figure 6.** (a) Velocity estimates for EHA with leakage faults,  
(b) Acceleration estimates with leakage faults.



280

281

**Figure 7.** Model probability weights.



282 **Figure 8.** The differences between SVSF and SMM-SVSF in terms of (a) Innovation squared,  
 283 (b) Error squared.

284 **Table 5.** RMSE results for SVSF and SMM-SVSF for scenario with leakage faults.

<b>Filter</b>	<b>Position (m)</b>	<b>Velocity (m/s)</b>	<b>Acceleration (m/s<sup>2</sup>)</b>	<b>Differential Pressure (Pa)</b>
<b>SVSF</b>	0.0003101	0.0091966	0.002810	0.001002
<b>SMM-SVSF</b>	0.0001828	0.0000799	0.000712	0.001002

285

286 The SMM-SVSF's ability to determine system modes can be seen in Figure 7, which shows  
 287 the weights of each system mode used to calculate the estimate. Throughout the entire experiment,  
 288 the SMM-SVSF filter calculates at least an 80% probability of the correct operating mode at every  
 289 stage of operation. The figure shows clear transitions from normal operation, to minor leakage, to  
 290 major leakage at 3 seconds and 6 seconds respectively. The innovation squared (IS), and error  
 291 squared (ES) are calculated and shown in Figure 8. These two compare the a priori and the a  
 292 posteriori squared errors between the two algorithms, respectively. Moreover, they show the  
 293 existence subspaces around the estimates in both prediction and update steps. From the figure, it

294 was easily obtained that the SMM-SVSF is more stable compared to the classical SVSF, and  
295 estimates are smoother with no chattering in SMM-SVSF compared to SVSF. The error of the  
296 classical SVSF in both steps increases due to introducing the faults, and it spikes when the actuator  
297 changes direction. In addition, the RMSE values in Table 5 show that the SMM-SVSF significantly  
298 reduces the errors in estimating the position, velocity, and acceleration.

## 299 **6. Conclusions**

300 This paper introduced the combination of the Smooth Variable Structure Filter and Static  
301 Multiple Mode estimation strategies to create an adaptive filtering method, SMM-SVSF, that can  
302 be used in fault and diagnosis applications. A brief background was provided on the estimation  
303 theory up to and including the sliding innovation filter. The SVSF was also included. The SMM-  
304 SVSF was tested on an Electro-Hydrostatic actuator. The filter performed well for this particular  
305 EHA model due to two main factors: the system parameters of the different leakage modes vary  
306 significantly enough for mode differentiation using the SMM method, and the system and  
307 measurement noise covariances are well-known. This paper demonstrates that the addition of  
308 SMM to the SVSF strategy improves overall estimation process for a system with multiple  
309 operating modes, and thereby creates an adaptive SVSF. This can be observed from the results,  
310 where the root mean squared errors were reduced by 41%, 99% and 75% for the position, velocity  
311 and acceleration estimated states when the SMM-SVSF is applied rather than SVSF. Potential  
312 future work will incorporate additional operating modes such as friction faults as well as the  
313 mixing of several different operating modes.

314

315

- [1] B. Ristic, S. Arulampalam and N. Gordon, *Beyond the Kalman Filter: Particle Filters for Tracking Applications*, Boston: Artech House, 2004.
- [2] M. Avzayesh, M. Abdel-Hafez, M. AlShabi and S. Gadsden, "The smooth variable structure filter: A comprehensive review. (2021) 110, art. no. 102912. DOI: 10.1016/j.dsp.2020.102912," *Digital Signal Processing*, vol. 110, 2021.
- [3] S. A. Gadsden, "Smooth Variable Structure Filtering: Theory and Applications," McMaster University, Hamilton, 2011.
- [4] H. H. Afshari, S. A. Gadsden and S. R. Habibi, "Gaussian Filters for Parameter and State Estimation: A Review of Theory and Recent Trends," *Signal Processing*, vol. 135, no. C, pp. 218-238, 2017.
- [5] V. I. Utkin, "Variable Structure Systems With Sliding Mode: A Survey," *IEEE Transactions on Automatic Control*, vol. 22, pp. 212-222, 1977.
- [6] V. I. Utkin, *Sliding Mode and Their Application in Variable Structure Systems*, English Translation ed., Mir Publication, 1978.
- [7] A. F. Fillipov, "Differential Equation with Discontinuous Right Hand Side," *American Mathematical Society Transactions*, vol. 62, 1969.
- [8] V. Utkin, *Sliding Modes in Control Optimization*, New York: Springer-Verlag, 1992.
- [9] J. J. E. Slotine, J. Hedrick and E. Misawa, "On Sliding Observers for Nonlinear Systems," *ASME Journal of Dynamic Systems, Measurement and Control*, vol. 109, no. 3, pp. 245-252, September 1987.
- [10] J. J. E. Slotine and W. Li, *Applied Nonlinear Control*, Englewood Cliffs, NJ: Prentice-Hall, 1991.
- [11] S. A. Gadsden and A. S. Lee, "Advances of the Smooth Variable Structure Filter: Square-Root and Two-Pass Formulations," *Journal of Applied Remote Sensing*, vol. 11, no. 1, pp. 1-19, 2017.
- [12] M. Al-Shabi, "The General Toeplitz/Observability SVSF," Hamilton, Ontario, 2011.
- [13] C. Milosavljevic, "General Conditions for the Existence of a Quasi-Sliding Mode on the Switching Hyperplane in Discrete Variable Structure Systems," *Automatic Remote Control*, vol. 46, pp. 307-315, 1985.
- [14] K. Furuta, "Sliding Mode Control of a Discrete System," *Systems Control Letters*, vol. 14, pp. 145-152, 1990.
- [15] S. Z. Sarpurk, Y. I Stefanopoulos and O. Kaynak, "On the Stability of Discrete-Time Sliding Mode Control Systems," *IEEE Transactions on Automatic Control*, Vols. AC-32, no. 10, pp. 930-932, October 1987.

- [16] S. K. Spurgeon, "Sliding Mode Observers: A Survey," *International Journal of Systems Science*, pp. 751-764, 2008.
- [17] S. H. Qaiser, A. I. Bhatti, M. Iqbal, R. Samar and J. Qadir, "Estimation of Precursor Concentration in a Research Reactor by Using Second Order Sliding Mode Observer," *Nuclear Engineering and Design*, vol. 239, pp. 2134-2140, 2009.
- [18] S. Qaiser, A. Bhatti, R. Samar, M. Iqbal and J. Qadir, "Higher Order Sliding Mode Observer Based Estimation of Precursor Concentration in a Research Reactor," in *4th IEEE Conference on Emerging Technologies*, 208.
- [19] C. Edwards and S. Spurgeon, "On the Development of Discontinuous Observers," *International Journal of Control*, vol. 59, pp. 1211-1229, 1994.
- [20] J. J. E. Slotine, J. Hedrick and E. Misawa, "On Sliding Observers for Nonlinear Systems," in *American Control Conference*, Seattle, Washington, 1986.
- [21] B. Walcott and S. Zak, "State Observation of Nonlinear Uncertain Dynamical Systems," *IEEE Transactions on Automatic Control*, Vols. AC-32, no. 2, pp. 166-170, February 1987.
- [22] B. Walcott, M. Corless and S. Zak, "Comparative Study of State Observation Techniques," *International Journal of Control*, vol. 45, no. 6, pp. 2109-2132, June 1987.
- [23] C. Tan and C. Edwards, "Sliding Mode Observers for Robust Detection and Reconstruction of Actuator and Sensor Faults," *International Journal of Robust and Nonlinear Control*, vol. 13, no. 1, pp. 443-463, January 2003.
- [24] S. R. Habibi, "The Smooth Variable Structure Filter," *Proceedings of the IEEE*, vol. 95, no. 5, pp. 1026-1059, 2007.
- [25] S. A. Gadsden, "Smooth Variable Structure Filtering: Theory and Applications," McMaster University (PhD Thesis), Hamilton, Ontario, 2011.
- [26] S. A. Gadsden, S. R. Habibi and T. Kirubarajan, "Kalman and Smooth Variable Structure Filters for Robust Estimation," *IEEE Transactions on Aerospace and Electronic Systems*, vol. 50, no. 2, pp. 1038-1050, 2014.
- [27] S. A. Gadsden and S. R. Habibi, "Derivation of an Optimal Boundary Layer Width for the Smooth Variable Structure Filter," in *ASME/IEEE American Control Conference (ACC)*, San Francisco, California, 2011.
- [28] S. A. Gadsden and S. R. Habibi, "A New Robust Filtering Strategy for Linear Systems," *ASME Journal of Dynamic Systems, Measurement, and Control*, vol. 135, no. 1, 2013.
- [29] S. A. Gadsden, M. Al-Shabi and S. R. Habibi, "Estimation Strategies for the Condition Monitoring of a Battery System in a Hybrid Electric Vehicle," *ISRN Signal Processing*, 2011.

- [30] J. Goodman, J. Kim, A. S. Lee and S. A. Gadsden, "A Variable Structure-Based Estimation Strategy Applied to an RRR Robot System," *Journal of Robotics, Networking and Artificial Life*, vol. 4, no. 2, pp. 142-145, 2017.
- [31] J. Kim, S. Bonadies, C. Eggleton and S. A. Gadsden, "Cooperative Robot Exploration Strategy Using an Efficient Backtracking Method for Multiple Robots," *ASME Journal of Mechanisms and Robotics*, vol. 10, no. 6, 2018.
- [32] M. Al-Shabi, S. A. Gadsden and S. R. Habibi, "Kalman Filtering Strategies Utilizing the Chattering Effects of the Smooth Variable Structure Filter," *Signal Processing*, vol. 93, no. 2, pp. 420-431, 2013.
- [33] H. H. Afshari, "The 2nd-Order Smooth Variable Structure Filter (2nd-SVSF) for State Estimation: Theory and Applications," McMaster University (PhD Thesis), Hamilton, Ontario, 2014.
- [34] S. A. Gadsden and A. S. Lee, "Advances of the Smooth Variable Structure Filter: Square-Root and Two-Pass Formulations," *Journal of Applied Remote Sensing*, vol. 11, no. 1, 2017.
- [35] M. Al-Shabi and A. Elnady, "Recursive Smooth Variable Structure Filter for Estimation Processes in Direct Power Control Scheme Under Balanced and Unbalanced Power Grid," *IEEE Systems Journal*, vol. 14, no. 1, pp. 971-982, 2019.
- [36] S. A. Gadsden and M. Al-Shabi, "The Sliding Innovation Filter," *IEEE Access*, vol. 8, pp. 96129-96138, 2020.
- [37] A. Lee, S. Gadsden and M. AlShabi, "An Adaptive Formulation of the Sliding Innovation Filter," *IEEE Signal Processing Letters*, vol. 28, pp. 1295-1299, 2021.
- [38] M. AlShabi, S. Gadsden, M. El Haj Assad and B. Khuwaileh, "A multiple model-based sliding innovation filter.," in *SPIE, Proceedings Volume 11756, Signal Processing, Sensor/Information Fusion, and Target Recognition XXX*, 2021.
- [39] M. AlShabi, S. Andrew Gadsden, M. El Haj Assad, B. Khuwaileh and S. Wilkerson, "Application of the sliding innovation filter to unmanned aerial systems.," in *SPIE, Proceedings Volume 11758, Unmanned Systems Technology XXIII*, 2021.
- [40] S. A. Gadsden, S. R. Habibi and T. Kirubarajan, "Kalman and Smooth Variable Structure Filters for Robust Estimation," *IEEE Transactions on Aerospace and Electronic Systems*, vol. 50, no. 2, pp. 1038-1050, 2014.
- [41] S. A. Gadsden, M. Al-Shabi, I. Arasaratnam and S. R. Habibi, "Combined Cubature Kalman and Smooth Variable Structure Filtering: A Robust Estimation Strategy," *Signal Processing*, vol. 96, no. B, pp. 290-299, 2014.
- [42] T. Q. S. Truong, "Exploration of Adaptive Filters for Target Tracking in the Presence of Model Uncertainty," Commonwealth of Australia, Rockingham, 2010.
- [43] S. A. Gadsden, Y. Song and S. R. Habibi, "Novel Model-Based Estimators for the Purposes of Fault Detection and Diagnosis," *IEEE/ASME Transactions on Mechatronics*, vol. 18, no. 4, 2013.

- [44] E. M and N. Sepehri, "Controller Design and Stability Anaylysis of Ouput Pressure Regulation in Electrohydrostatic Actuators," *AMSE, Journal of Dynamic Systems, Measurement, and Control*, vol. 141, no. 041008-1, 2019.
- [45] A. Maddahi, W. Kinsner and N. Sepehri, "Internal Leakage Detection in Electrohydrostatic Actuators Using Multiscale Analysis of Experimental Data," *IEEE Transactions on Instrumentation and Measurement*, vol. 65, no. 12, pp. 2734-2747, 2016.
- [46] H. H. Afshari, S. A. Gadsden and S. R. Habibi, "Robust Fault Diagnosis of an Electro-Hydrostatic Actuator using the Novel Optimal Second-Order SVSF and IMM Strategy," *International Journal of Fluid Power*, vol. 15, no. 3, pp. 181-196, 2014.
- [47] S. A. Gadsden and T. Kirubarajan, "Development of a variable structure-based fault detection and diagnosis strategy applied to an electromechanical system," *Proceedings of SPIE 10200, Signal Processing, Sensor/Information Fusion, and Target Recognition* , vol. XXVI, 2017.

317

318